RESEARCH ARTICLE

Proteomic analysis of the effects of the immunomodulatory mycotoxin deoxynivalenol

André Nogueira da Costa[1], Renée S. Mijal[1], Jeffrey N. Keen[2], John B. C. Findlay[2,3] and Christopher P. Wild[1]**

[1] Molecular Epidemiology Unit, Division of Epidemiology, Leeds Institute of Genetics, Health and Therapeutics, University of Leeds, Leeds, UK
[2] Institute of Membrane and Systems Biology, Faculty of Biological Sciences, Leeds Institute of Genetics, Health and Therapeutics, University of Leeds, Leeds, UK
[3] Marie Curie Laboratory for Membrane Proteins, Department of Biology, NUI Maynooth, Co. Kildare, Ireland

Received: September 10, 2010
Revised: January 22, 2011
Accepted: January 31, 2011

The mycotoxin deoxynivalenol (DON) contaminates cereals worldwide and is a common contaminant in the Western European diet. At high doses, DON induces acute gastrointestinal toxicity; chronic, low-dose effects in humans are not well described, but immunotoxicity has been reported. In this study, 2-DE was used to identify proteomic changes in human B (RPMI1788) and T (JurkatE6.1) lymphocyte cell lines after exposure to minimally toxic concentrations (up to 500 ng/mL) for 24 h. Proteins which changed their abundance post treatment, by a greater than 1.4-fold change reproducible in three separate experiments consisting of 36 gels in total, are ubiquitin carboxyl-terminal hydrolase isozyme L3, proteasome subunit β type-4 and α type-6, inosine-5′-monophosphate dehydrogenase 2, GMP synthase, microtubule-associated protein RP/EB family member 1 (EB1), RNA polymerases I, II, III subunit ABC1, triosephosphate isomerase and transketolase. Flow cytometry was used to validate changes to protein expression, except for EB1. These findings provide insights as to how low-dose exposure to DON may affect human immune function and may provide mechanism-based biomarkers for DON exposure.

Keywords:
Animal proteomics / Biomarkers / 2-DE / DON / Mycotoxins

1 Introduction

The mycotoxin deoxynivalenol (DON) is a common contaminant of cereals such as wheat, corn and barley [1]. As a member of the trichothecene family of mycotoxins, DON is a toxic secondary metabolite that can be produced by strains of *Fusarium*, *Stachybotrys* and other saprophytic and plant parasitic fungi. Common symptoms that characterize high-dose exposure to DON include gastrointestinal tract toxicity, emetic effects, decreased weight gain and reduced food intake [2, 3]. Recently, studies in cell culture and animal models demonstrated that at lower concentrations DON might also modify immune function, acting as both immunostimulatory and immunosuppressive agent [4, 5].

At a cellular and molecular level, different mechanisms have been proposed to explain the toxicity of DON. The

Correspondence: Dr. André Nogueira da Costa, Molecular Carcinogenesis Group, Section of Mechanisms of Carcinogenesis, International Agency for Research on Cancer, 150 Cours Albert-Thomas 69372 Lyon Cedex 08, France
E-mail: dacostaa@fellows.iarc.fr
Fax: +33-472738322

Abbreviations: AU, arbitrary units; **DON,** deoxynivalenol; **G3P,** glyceraldehyde-3-phosphate; **GMPS,** GMP synthase; **IMDH2,** inosine-5′-monophosphate dehydrogenase 2; **EB1,** microtubule-associated protein RP/EB family member 1; **MTT,** 3-(4,5-dimethylthiazolyl-2)-2,5-diphenyltetrazolium bromide; **PPP,** pentose phosphate pathway; **PSA6,** proteasome subunit α type-6; **PSB4,** proteasome subunit β type-4; **TIM,** triosephosphate isomerase; **TK,** transketolase; **UCHL3,** ubiquitin carboxyl-terminal hydrolase isozyme L3

*Current addresses: Christopher P. Wild, International Agency for Research on Cancer, 150 Cours Albert Thomas, 69372 Lyon CEDEX 08, France;
Renée S. Mijal, Department of Preventive Medicine and Public Health, University of Kansas Medical School, Kansas City, KS 66160, USA

primary mode of action of DON may be the inhibition of protein systems through binding to eukaryotic ribosomes [6, 7]. Alternatively, DON toxicity may also arise through: impairment of membrane function, disruption of intercellular communication, deregulation of calcium homeostasis and early alterations in cell signaling mediated through mitogen-activating protein kinase(s) (MAPK)-dependent pathways [6, 7].

Since the mid-20th century, studies have implicated mycotoxins in food poisoning outbreaks and DON has been one of the dietary contaminants found at highest concentrations [8, 9]. Despite these observations the etiology of many outbreaks remains unknown. Biomarkers promise to provide more objective measures of DON exposure in order to explore disease associations, but few such studies have been conducted although exposure of DON affects immune cells immunoglobulins and pro-inflammatory cytokines [10–12]. The identification of biomarkers of exposure has focused on the urinary levels of the parent compound and its glucuronide conjugate [13, 14]. Recent studies in the UK have revealed that the majority of people have detectable DON in their urine, some at levels which result from exposures exceeding the provisional maximum tolerable daily intake (PMTDI) of 1 μg/kg body weight/day [15].

The application of a gel-based proteomics approach to develop potential mechanism-based biomarkers for DON is one approach. In this respect, we have compared protein expression in human B (RPMI 1788) and T (Jurkat E6.1) lymphocyte cell lines exposed to DON at a maximum concentration of 500 ng DON/mL. These cell types are good representations of major cellular components of the adaptive immune response and have been used extensively to study modulation of the immune system [16–20]. In vitro cell line models were selected due to the purity of the cell preparations and the ability to match quantitative levels of DON exposure with biological effects as a first step to subsequent studies in humans where dietary exposures are difficult to quantify and variable. A panel of nine proteins, ubiquitin carboxyl-terminal hydrolase isozyme L3 (UCHL3), proteasome subunit β type-4 (PSB4) and α type-6 (PSA6), inosine-5′-monophosphate dehydrogenase 2 (IMDH2), GMP synthase (GMPS), microtubule-associated protein RP/EB family member 1 (EB1), RNA polymerases I, II, III subunit ABC1, triosephosphate isomerase (TIM) and transketolase (TK), exhibited validated altered expression across these cell lines and may represent valuable biomarkers to understand how low dose, chronic exposure to DON affects human immune function.

2 Materials and methods

2.1 Reagents

RPMI 1640 (+L-glutamine) medium was from Gibco (Invitrogen, Paisley, UK); DON, 3-(4,5-dimethylthiazolyl-2)-2,5-diphenyltetrazolium bromide (MTT), gelatine from cold water fish skin and protease inhibitor cocktail were supplied by Sigma-Aldrich (Dorset, UK); ProteoExtract Protein Precipitation Kit was from Calbiochem (Merck Chemicals, Nottingham, UK); ampholytes and 24 cm pH 3–10 nonlinear IPG strips were from Bio-Rad (Hertfordshire, UK); SYPRO Ruby stain was from Invitrogen; ACN, formic acid and trifluoroacetic acid used for MS analysis or sample preparation were of HPLC quality (Fisher Scientific, Leicestershire, UK); HPLC-grade water was prepared with a Neptune Ultimate System (Purite, Oxon, UK); sequencing grade trypsin for protein digestion was from Promega (Southampton, UK); goat anti-mouse IgG-PE (phycoerythrin) was from Santa Cruz Biotechnology (Heidelberg, Germany); IMDH2 mouse monoclonal antibody, PSB4 mouse monoclonal antibody, PSA6 mouse polyclonal antibody, UCHL3 mouse monoclonal antibody, GMPS mouse monoclonal antibody, EB1 mouse monoclonal antibody, TIM mouse monoclonal antibody, TK mouse polyclonal antibody and RNA polymerases I, II, III subunit ABC1 polyclonal antibody were from Abnova (Taiwan).

2.2 Cell culture and DON treatment

Human B lymphocyte cell line (RPMI 1788, ECACC, UK) and human T lymphocyte cell line (Jurkat E6.1, ECACC) were grown at 37°C in a humidified atmosphere consisting of 5% CO_2 air, in RPMI 1640 (+L-glutamine) medium supplemented with 20% v/v heat-inactivated FCS or 10% v/v heat-inactivated FCS, respectively. Cells were kept in the exponential growth phase, at a concentration of 3×10^5 cells/mL. Stock solutions and subsequent working solutions of DON were prepared in absolute ethanol. Working solutions of DON were prepared with a maximum concentration of 0.05% absolute ethanol. Vehicle control cells were prepared in the same manner as DON-treated samples including the addition of the vehicle control (0.05% ethanol), instead of DON. Cell treatments were conducted in flat bottom 96-well and 12-well plates (Fisher Scientific). Cells were treated with DON for a period of 24 h, with concentrations ranging from 0 to 500 ng DON/mL. At the end of the incubation period, cells were either stored at −80°C or immediately used for cytotoxicity measurements, proteomic studies and flow cytometry experiments.

2.3 Measurement of cytotoxicity

The MTT assay was utilized to evaluate toxicity. Cells were grown in flat bottom 96-well plates at a concentration of 6×10^5 cells/mL per well with DON for a period of 24 h, in a humidified atmosphere consisting of 5% CO_2 air, at 37°C. At the end of the treatment period, 10 μL of MTT was added to the cells and the plates were incubated for 4 h. Subsequently, 100 μL of 10% w/v SDS in 0.01 M HCl was added

and the plate incubated overnight. On the following day, absorbance levels were recorded at 540 and 690 nm using an iEMS Reader MF (Labsystems, Cambridge, UK). Each plate contained a positive control consisting of cells incubated with 9% v/v Triton X-100 prior to the addition of MTT. Reproducibility was assured by conducting five independent experiments with each sample repeated in triplicate.

2.4 Cell lysis and 2-DE

Cells were lysed with 200 μL of lysis buffer that included 7 M urea, 2 M thiourea, 4% w/v 3-CHAPS, 64 mM DTT and 1% v/v protease inhibitor cocktail (Sigma-Aldrich). The lysates were centrifuged at $13\,250 \times g$ for 15 min and the supernatant treated with ProteoExtract Protein Precipitation Kit (Calbiochem, Merck Chemicals) according to the manufacturer's protocol. After resuspending the protein pellets in lysis buffer, the lysate was centrifuged at $13\,250 \times g$ for 15 min and the supernatant collected. The protein concentration of the supernatants was determined using the Bradford assay (Bio-Rad). An aliquot, equivalent to 350 μg of total protein, of each supernatant was applied to a 24 cm pH 3–10 non-linear IPG strip overnight, allowing for the passive rehydration of the IEF strips. IEF was carried out using the ProteanIEF system (Bio-Rad) with the following program: (i) 250 V, 8 h; (ii) 10 000 V, 2.5 h; (iii) 60 000 Vh, at a limit of 10 000 V; (iv) 500 V until equilibration. The first equilibration step was carried out by washing the strips for 15 min in a buffer containing 2% w/v DTT, 6 M urea, 0.05 M Tris-HCl (pH 8.8), 2% w/v SDS and 20% v/v glycerol. The second equilibration step (15 min) used the same buffer but with 2.5% w/v iodoacetamide replacing DTT. For the second dimension, strips were transferred onto SDS-PAGE gels containing 10% w/v acrylamide, prepared with a multicasting chamber (Bio-Rad). Migration was carried out for 6 h at a constant voltage of 200 V in a Protean Plus DoDecaCell tank (Bio-Rad), cooled by water flow maintained at 10°C. Gels were incubated in a 50% v/v methanol, 7% v/v acetic acid solution for 1 h. Gels were stained overnight with SYPRO® Ruby, then washed for 30 min in 10% v/v methanol, 7% v/v acetic acid and subsequently twice in ultra-pure water for 5 min. Reproducibility was assured conducting three independent experiments comprising triplicate samples for each condition ($n = 6$).

2.5 Image analysis

Gels were scanned using an FX Pro Plus imager (Bio-Rad) and the images analyzed using PDQuest software version 7.3.1 (Bio-Rad) as indicated in Fig. 2. For each cell line, three independent experiments consisting of triplicate gels for each condition were analyzed; in total 36 gels. Using the PDQuest software, only significant changes of at least 1.4-fold seen in each gel on each occasion were treated as meaningful. The quantitation and statistical analysis of changes to spot intensity are achieved by (i) generation of an optical density reading for each spot detected; (ii) automatic determination of spot density; (iii) generation of Gaussian modeling for precise identification and quantitation of spots; (iv) automatic determination of SD and coefficient of variation and (v) conduction of statistical analysis based on the number of replicate groups and the number of gels per group. Each set of six gels was analyzed twice using the software.

2.6 Identification of proteins using peptide mass fingerprinting

2.6.1 Sample preparation

Selected spots were excised and transferred into a 96-well plate using the ProteomeWorks SpotCutter robot (Bio-Rad). The excised pieces of gel were processed automatically by a MassPREP workstation (Waters, Hertfordshire, UK) performing the following steps: washing/destaining (1:1 mixture of 50% v/v ACN and 50 mM ammonium bicarbonate), reduction (DTT 10 mM, ammonium bicarbonate 100 mM), alkylation (iodoacetamide 55 mM, ammonium bicarbonate 100 mM), ACN dehydration, digestion (trypsin 6 ng/μL), extraction from the gel (1% v/v formic acid, 2% v/v ACN) and finally spotting of the peptides and matrix (CHCA, 2 mg/mL in 50% v/v ACN, 0.1% v/v trifluoroacetic acid) on the MALDI plate (Waters, Manchester, UK).

2.6.2 MALDI-TOF MS analysis

A MALDI L/R MALDI-TOF mass spectrometer (Waters), operating in positive ion reflectron mode, was used to obtain the peptide mass spectra. Spectra were processed and calibrated externally with a tryptic digest of alcohol dehydrogenase. Internal calibration was performed using a single trypsin autodigestion peak (m/z 2211.105) as a Lockmass point. Monoisotopic peak masses presenting m/z ratios from 900 to 2800 were submitted to the MASCOT search engine (Matrix Science, London, UK; http://www.matrixscience.com) in order to identify proteins.

2.6.3 Database search for protein identification

Searches were generally performed using the Swiss-Prot database, up to one missed cleavage site, mass error of 200 ppm and variable modifications of carbamidomethyl (C) and oxidation (M). Further details of parameters used and any variations are detailed in the Supporting Information. Protein identifications were accepted on the following criteria: five or more matching peptides; a

MOWSE score of more than 56; sequence coverage greater than 20%. Details of peptide mass lists used for searches and proteins identified are supplied in the Supporting Information Table T2.

2.7 Identification of proteins using nano-HPLC-Chip Ion Trap MS/MS

2.7.1 Sample preparation

Selected spots were transferred to a siliconized tube and incubated with 50 μL of a 100 mM DTT:50 mM ammonium bicarbonate solution for 1 h at 56°C. After cooling to room temperature, the DTT:ammonium bicarbonate solution was replaced by 50 μL of a 55 mM iodoacetamide:50 mM ammonium bicarbonate solution for 45 min at RT in the dark and vortexed every 15 min. Samples were then washed for five times in 50 mM ammonium bicarbonate and/or 50% v/v ACN. Supernatants were discarded and tubes were vacuum centrifuged at 200 mBar, for 30 min at 40°C, followed by digestion with sequencing grade trypsin (20 μg/mL) in 50 mM ammonium bicarbonate at 37°C for 1 h. The trypsin/ammonium bicarbonate solution was then replaced with 30 μL of 50 mM ammonium bicarbonate and tubes were left at 37°C overnight. On the following day, samples were centrifuged for 1 min at 13 250 × *g* and 2 μL aliquots of each tryptic digest were analyzed by nano-HPLC-Chip Ion Trap MS/MS.

2.7.2 HPLC-Chip-MS/MS ANALYSIS

HPLC-Chip-MS/MS analysis was performed as described earlier [21]. Particular methodological steps are as follows: the chromatographic chip incorporated a 40-nL enrichment column, a 150/75-μm analytical column packed with Zorbax 300SB-C18 5 μm particles and a nanospray needle. Solvents used were A, 100% water, 0.1% v/v formic acid and B, 90% v/v ACN, 10% v/v water and 0.1% v/v formic acid. The capillary pump delivered an isocratic 100% A solvent phase at 4 μL/min. The nano-LC used 95% solvent A and 5% solvent B at all times unless generating a gradient, the flow rate in all instances being 0.6 μl/min. The nano-pump gradient program was as follows: 5% solvent B (0 min), 70% solvent B (0–7 min), 100% solvent B (8–10 min), to 5% solvent B for 10 min at 0.6 μL/min. Flows from the capillary and nano-pump were controlled using nano-flow sensors and active splitters. The drying gas temperature was 300°C, the flow was 4 L/min (nitrogen) and data acquisition occurred in positive ionization mode. Capillary voltage was 1800 V with endplate offset of 500 V. The recorded mass range was 200–2200 m/z, with a target mass of 700 m/z, an average of two spectra, ICC target 500 000 and maximum accumulation time was 200 ms. The MS/MS analyses were performed in the Auto MS(n) mode with the following criteria: fragmentation amplitude at 1 V, number of MS/MS stages was 2, number of precursor ions selected for MS/MS during each scan was 2 and doubly charged ions were selected.

2.7.3 Database search for protein identification

Database search for protein identification was performed as described earlier [21]. The whole NCBInr database was searched using the Agilent SpectrumMill software (Rev A.03.03.080). Raw MS/MS data files were analyzed to extract high-quality experimental fragmentation spectra. The MS/MS raw file data extractor selected and merged spectra with the same precursor ion within 61.4 m/z and within a time frame of 420 s. Precursor charge of up to 3 was selected, precursor ions required a minimum S/N value of 25 and the C12 peaks were determined by the Data Extractor. Searches were performed using the NCBInr protein database (taxonomy: human), tryptic peptides with a mass tolerance of ± 1.2 Da for precursor ions and a tolerance of ± 0.7 Da for fragment ions were searched; one missed cleavage was allowed. Modifications allowed for were carbamidomethyl (C) and oxidation (M). For each identified peptide, the distinctive peptide number, the peptide search score and the percentage scored peak intensity (SPI) were calculated.

2.8 Flow cytometry confirmation

Cells were fixed in 1% v/v paraformaldehyde and subsequently resuspended in PBS. Cell concentration was adjusted to 2×10^6 cells/mL and an aliquot of 500 μL was permeabilized in 2 × permeabilization buffer (PBS, 2.5 mM EDTA, 4% v/v fish skin gelatin and 1% v/v Triton X-100). Permeabilized cells were incubated with mouse anti-human IMDH2, PSB4, PSA6, UCHL3, GMPS, EB1, TIM, TK and RNA polymerases I, II, III subunit ABC1 (Abnova) as primary antibody for 1 h on ice and subsequently washed in cold PBS and centrifuged. Cells were then resuspended in 200 μL of 1 × permeabilization buffer and incubated with a goat anti-mouse IgG-PE-conjugated secondary antibody (Santa Cruz Biotechnology) on ice for 1 h. Prior to analysis, cells were centrifuged, washed and resuspended in 400 μL of PBS. Flow cytometry quantitative analysis was conducted using a FACSCalibur (Becton Dickinson, UK). Analysis of data was performed using the CellQuest™ Software (Becton Dickinson). Results are presented in arbitrary units (AU) resulting from the ratio between the mean fluorescence intensity (MFI) of unstained samples (negative control samples) and stained samples (vehicle control and treated samples). Each experiment contained a negative control consisting of untreated Jurkat E6.1 or RPMI 1788 cells. While vehicle control and treated samples were incubated with respective antibodies, negative control samples were

not stained with any antibodies. At the end of the experimental procedure, negative control samples were analyzed in the same manner as vehicle control and treated samples. Reproducibility was assured by conducting three independent experiments with each sample repeated at least three times.

2.9 Statistical analysis

Cytotoxicity results are presented as mean ± SD. Overall experimental reproducibility was assured by conducting five independent experiments consisting of triplicate repeats of vehicle control samples and treated samples. Overall experimental reproducibility of 2-DE gel results was assured by conducting three independent experiments comprising triplicate repeats of vehicle control gels and treated gels. In total, 18 gels were run for each cell line. Statistical differences were evaluated with a Student's *t*-test, $p < 0.01$ using the statistical package included in PDQuest software version 7.3.1 (Bio-Rad). Flow cytometry experiments are presented as mean of AU ± SD. Overall experimental reproducibility was assured by conducting three independent experiments consisting of at least three repeats of vehicle control samples and treated samples. For cytotoxicity and flow cytometry experimental approaches, differences were evaluated with a Student's *t*-test, $p < 0.02$ (SPSS 15.0, USA).

3 Results

3.1 Measurement of cytotoxicity

The cytotoxicity of DON (0–500 ng/mL over 24 h) was evaluated using the MTT assay for both Jurkat E6.1 and RPMI 1788 cells. The two cell lines differ in their sensitivity to DON (Fig. 1). In Jurkat E6.1 cells, toxicity levels above 20 and 40% were reached at 250 and 500 ng DON/mL, respectively. In contrast, RPMI 1788 cells appear to be less sensitive to DON as toxicity levels above 20% were only observed at 500 ng DON/mL. When compared to vehicle-treated cells these concentrations gave a statistically significant increase in toxicity ($p < 0.01$). Concentrations that gave greater than 20% toxicity in each cell line after 24-h treatments were utilized in the proteomics studies.

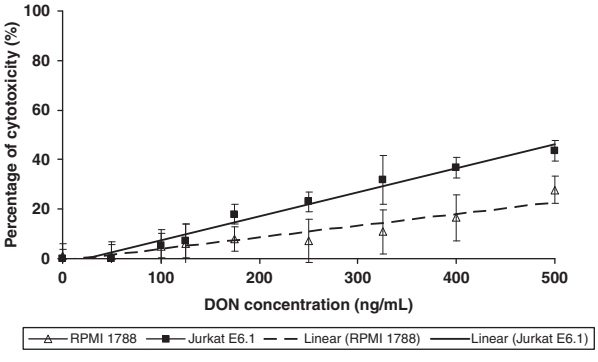

Figure 1. Cytotoxicity of DON in RPMI 1788 (triangle) and Jurkat E6.1 (square) cells measured by the MTT assay. The correlation coefficients (*r*) for the linear regression equations were calculated for each cell line (RPMI 1788, $r^2 = 0.8934$; Jurkat E6.1, $r^2 = 0.9779$). Each point represents the mean ± SD of 15 replicates.

3.2 2-DE

For Jurkat E6.1 and RPMI 1788 cells, control samples were exposed to ethanol at 0.05% (vehicle control) and treated samples were exposed to 250 and 500 ng DON/mL, respectively. Soluble proteins (350 μg) from control and treated samples were subjected to 2-DE in the range of pH 3–10. After the second dimension (10% gels), gels were stained with SYPRO Ruby (Fig. 2). Three sets of six gels were run for both types of cell line. Each set consisted of three control sample gels and three treated sample gels; in total, 18 gels for each type of lymphocyte. An average of 1200 spots was detected per gel. Five spots showed reproducible expression changes in Jurkat E6.1 cells and four spots in RPMI 1788 cells (Supporting Information Fig. F1). Findings were reproducible across all gels within each experiment and in three separate experimental treatments ($p < 0.01$).

3.3 Protein identification

All nine proteins were identified using both MALDI-TOF MS and nano-HPLC-Chip Ion Trap MS (Table 1 and Supporting Information Table T1). In Jurkat E6.1 cells, UCHL3, PSB4, PSA6, IMDH2 and GMPS all exhibited upregulation. In RPMI 1788 cells, EB1 and RNA polymerases I, II and III subunit ABC1 were found to be upregulated, while TIM and TK were found to be downregulated. The proteins identified (Table 2) are involved in proteasomal degradation, morphological processes, metabolism regulation and transcription process.

3.4 Flow cytometry confirmation

Flow cytometry was utilized to confirm changes in protein expression of all proteins. Comparison between control and treated samples showed an upregulation of 1.4-, 1.3-, 1.5-, 1.3-, 1.2- and 1.3-fold for IMDH2, PSB4, PSA6, UCHL3, GMPS and RNA polymerases I, II, III subunit ABC1, respectively. We were not able to confirm changes to protein expression in EB1. TIM and TK were shown to be downregulated at 1.2- and 1.5-fold, respectively (Fig. 3, Supporting Information Table T3–T10). All experiments contained a

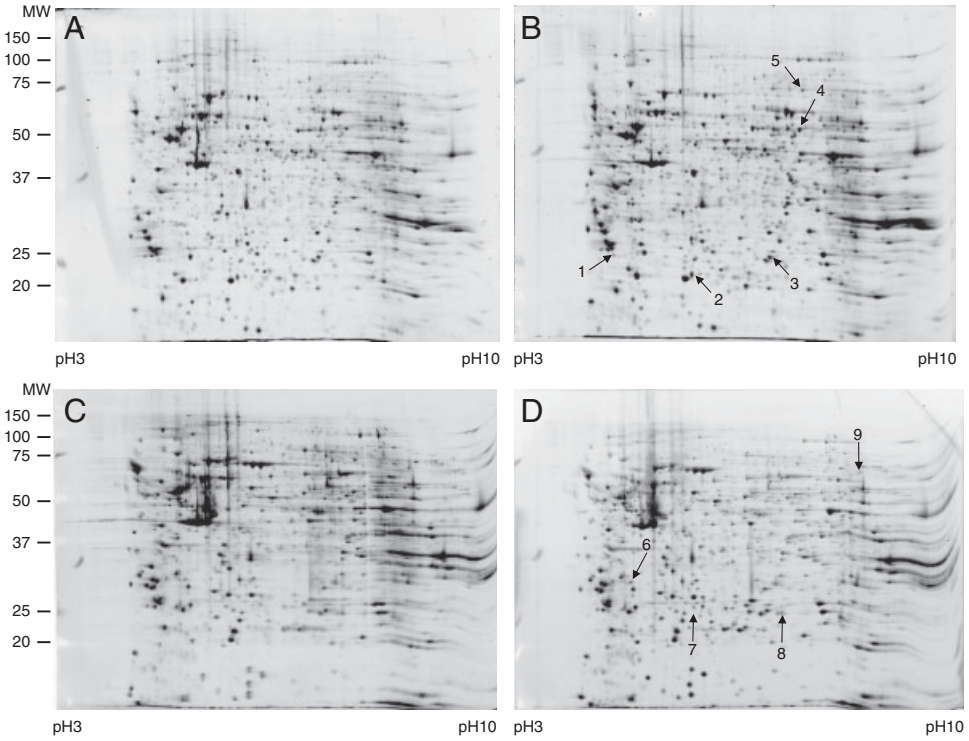

Figure 2. Image of representative 2-DE gels of (A) Jurkat E6.1 control cells, (B) Jurkat E6.1 treated cells at 250 ng DON/mL, (C) RPMI 1788 control cells and (D) RPMI 1788 treated cells at 500 ng DON/mL. All gels were stained with SYPRO Ruby. Molecular range from 250 to 10 kDa, p*I* range from 3 to 10. Highlighted are nine spots showing change in expression following DON exposure.

negative control to account for auto-fluorescence. The results are statistically significant ($p < 0.01$ or 0.02) and confirm the pattern of expression which was obtained using 2-DE.

4 Discussion

The search for valid biomarkers of exposure and/or effect associated with mycotoxins has resulted in the identification of useful and validated markers such as DON and its glucuronide (in the urine) [14]. However, no protein biomarkers have been identified to date but these would be valuable in providing mechanism-based indicators of exposure and effects. In this study, using Jurkat E6.1 and RPMI 1788 cells as models, we have identified candidate mechanism-based proteins associated with low-dose exposure to DON. Our first objective was to determine the ideal concentration and exposure period, which would allow the induction of changes to the proteome while limiting the levels of DON toxicity.

In this first analysis of the effects of DON on the proteome, we selected doses associated with modest (~20%) toxicity in Jurkat E6.1 and RPMI 1788 cells, 250 and 500 ng DON/mL, respectively; these doses correspond to the lower end of the range typically studied in vitro in relation to DON and its immune effects [12, 22].

Five proteins from Jurkat E6.1 cells and four proteins from RPMI 1788 cells displayed altered expression reproducibly across all sets of gels (Fig. 2).

4.1 Proteasomal degradation

Three proteins involved in the proteasome degradation pathway were identified as being upregulated in Jurkat E6.1 cells: UCHL3, PSB4 and PSA6. UCHL3 is a deubiquitination enzyme that has been associated with cell apoptosis in the retina, spermatogenesis, neurodegenerative diseases as well as membrane recycling of calcium channels [23–25]. Proteomic approaches have identified UCHL3 as a protein involved in malignant transformation in biopsies of cervical carcinoma associated with human papillomavirus and as a potential biomarker of exposure to the carcinogen anti-benzo[a]pyrene-7,8-dihydrodiol-9,10-epoxide [26, 27]. The upregulation of this protein could lead to higher protein degradation through the detachment of the polyubiquitin tags, in turn causing an increased number of unfolded polypeptides in the catalytic core of the proteasome. Such an increase could consequentially lead to a higher activity of the proteins that compose the 20S catalytic core.

Both PSB4 and PSA6 are part of the 20S catalytic core of the proteasome. β Subunits are characterized as containing

Table 1. Proteins exhibiting change in expression in Jurkat E6.1 lymphocytes (spots 1–5) and RPMI 1788 lymphocytes (spots 6–9), identified by MALDI-TOF MS and nano-HPLC-Chip Ion Trap MS

Spot	Protein identified	Identified in	Accession number	MALDI-TOF MS			nano-HPLC-Chip Ion Trap MS			Mw (kDa)	p*I*	Fold change	Regulation
				MOWSE score	Peptides matched	Sequence coverage (%)	MS/MS score	Peptides matched	Sequence coverage (%)				
1	UCHL3	Jurkat E6.1	P15374	81	6	40	126.80	7	40	26.2	4.84	1.5	Up
2	PSB4	Jurkat E6.1	P28070	85	7	36	75.85	5	24	29.2	5.72	1.8	Up
3	PSA6	Jurkat E6.1	P60900	157	12	53	158.67	9	42	27.4	6.34	1.4	Up
4	IMDH2	Jurkat E6.1	P12268	168	16	37	329.61	19	36	55.8	6.44	1.5	Up
5	GMPS (glutamine-hydrolyzing)	Jurkat E6.1	P49915	206	24	42	408.38	25	42	76.7	6.42	1.4	Up
6	EB1	RPMI 1788	Q15691	84	9	43	219.35	14	52	30	5.02	1.6	Up
7	DNA-directed RNA polymerases I, II, and III subunit RPABC1 (RNA polymerases I, II, III subunit ABC1)	RPMI 1788	P19388	108	9	40	165.61	11	49	24.7	5.69	1.4	Up
8	TIM	RPMI 1788	P60174	107	13	61	229.53	13	58	26.7	6.45	1.4	Down
9	TK	RPMI 1788	P29401	86	13	27	339.72	23	38	67.8	7.58	1.7	Down

Statistical significance was considered at $p \leq 0.01$ (*t*-test).

Table 2. Groupings of proteins based on putative function

Putative function	Proteins identified
Proteasome degradation	Ubiquitin carboxyl-terminal hydrolase isozyme L3
	Proteasome subunit beta type-4
	Proteasome subunit alpha type-6
Carbohydrate metabolism	Triosephosphate isomerase
	Transketolase
Nucleotide metabolism	Inosine-5′-monophosphate dehydrogenase 2
	GMP synthase [glutamine-hydrolyzing]
Regulation of transcription	DNA-directed RNA polymerases I, II, and III subunit RPABC1
Microtubule polymerization	Microtubule-associated protein RP/EB family member 1

the protease active sites, while the α subunits serve as docking domains for the regulatory particles and form a gate that blocks unregulated access of substrates to the central pore. Here, PSB4 and PSA6 were seen to be upregulated by DON, probably related to the increase in degradation of polypeptides in the catalytic core as suggested by the increase in UCHL3 activity. To date, no studies have associated these proteins to specific human T lymphocyte function. However, a recent study which analyzed the proteome of EL-4 cell line exposed to DON at a concentration of 0.5 μM, identified proteasome subunit α 1 as being upregulated. This study further supports the upregulation of the proteins that make up the 20S catalytic core of the proteasome as well as the effect of DON on proteasomal degradation [28].

It has been reported that the proteasome plays a critical role in the function of the adaptive immune system through degrading proteins of the invading pathogen into peptides that can then be displayed on the surface of antigen presenting cells [29]. Proteasomal activity has also been associated with the activation of NF-κB, a central transcription factor that regulates the expression of genes related to inflammation such as cytokines [29, 30]. Studies looking at the correlation between DON exposure and IFN-γ regulation have shown that DON contributes to the upregulation of this cytokine in macrophages, T cells and blood mononuclear cells [31, 32]. Subsequent studies have also associated DON exposure with activation of NF-κB and subsequent secretion of cytokines such as IL-8 in animals and human immortalized cells [33–35].

4.2 Nucleotide metabolism

IMDH2 (E.C. 1.1.1.205) and GMPS (E.C. 6.2.5.2) were both found to be upregulated in Jurkat E6.1 cells. Both proteins have been identified as enzymes in purine metabolism. Abnormal purine metabolism can lead to disorders, such as gout, Lesch-Nyhan syndrome and severe combined immunodeficiency disease [36]. Inosine-5′-monophosphate dehydrogenase (IMDH) is the rate-limiting enzyme in de novo synthesis of guanine nucleotides. Two closely related human IMDH isoforms, types 1 and 2, have been identified, type 2 being predominant isoform [37]. The enzyme catalyzes the conversion of inosine-5′-monophosphate to xanthine-5′-monophosphate using NAD as a cofactor and has been associated with maintaining the pools of guanine deoxyribonucleotides and ribonucleotides in the cell for DNA and RNA synthesis [38]. When inhibited, it has been associated with reduced lymphocyte proliferation and immunosuppression [39]. Studies conducted in lymphocytes isolated from peripheral blood mononuclear cells reported that IMDH2 expression is upregulated upon mitogen activation [40] and in cases of acute lymphoblastic leukemia elevated IMDH activity is associated with lymphoblasts which express elevated IMDH2 [41].

GMPS (glutamine-hydrolyzing) is involved in the purine metabolism pathway and is responsible for the production of guanosine-5′-monophosphate from xanthine-5′-monophosphate. Several studies looking have identified this enzyme as a potential target for anticancer and immunosuppressive therapies [42]. To date, scarce are the studies that have associated the activity of this enzyme with human lymphocyte function. The upregulation of GMPS could lead to an increase in inosine-5′-monophosphate and guanine nucleotides, as with an upregulation of IMDH2.

4.3 Carbohydrate metabolism

TK (E.C. 2.2.1.1) and TIM (E.C. 5.3.1.1) were both downregulated in RPMI 1788 cells after exposure to DON. TK is involved in the pentose phosphate pathway (PPP), which generates NADPH and synthesizes pentose sugars [43]. Together with transaldolase (TA), TK serves as a reversible link between the oxidative part of the PPP and glycolysis, allowing the cell to adapt to a variety of metabolic needs by feeding excess sugar phosphates into the main carbohydrate metabolic pathways [43]. Studies conducted in primary human leukocytes demonstrated that there are at least two variants of TK in human leukocytes and underline that thiamine deficiency induces tissue damage by down-regulating mRNA levels of TK [44, 45]. Metabolic profiling of Jurkat E6.1 cells has reinforced that TK and transaldolase activity are responsible for recycling pentoses in glycolysis while simultaneously contributing to the synthesis of ribose from glycolysis intermediates [46]. From this, we can postulate that a downregulation of TK induced by DON may influence the production of F6P and glyceraldehyde-3-phosphate (G3P) leading to a decrease in activity in both the oxidative and non-oxidative arms of PPP, in the glycolytic process and in purine, pyrimidine and histidine metabolism. It will be very relevant to underst and the effects of DON exposure directly on ribose-5-P

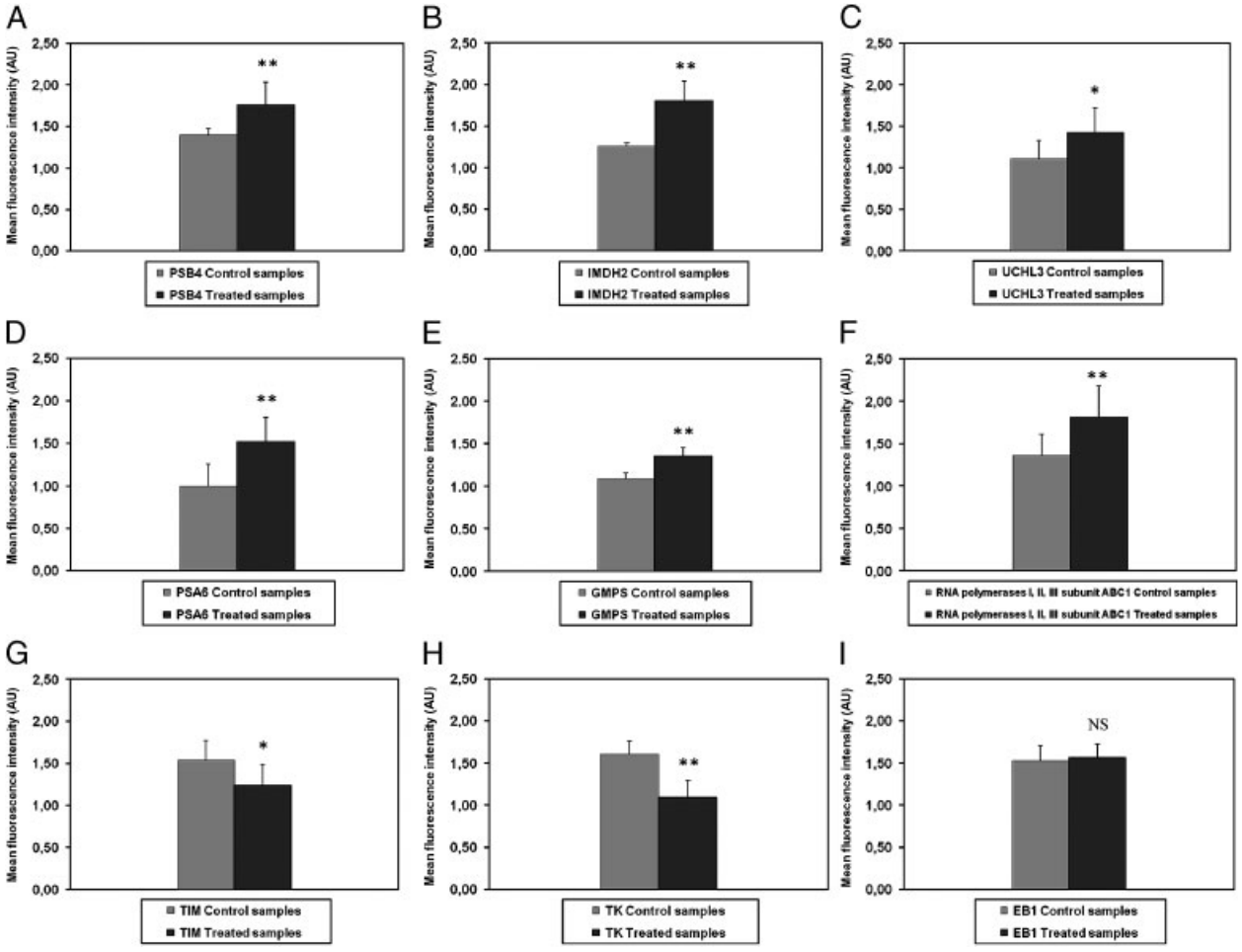

Figure 3. Quantitative confirmation of changes in (A) PSB4, (B) IMDH2, (C) UCHL3, (D) PSA6, (E) GMPS, (F) RNA polymerases I, II and III subunit ABC1, (G) TIM, (H) TK and (I) EB1 expression measured by flow cytometry. Each bar represents the mean AU $\pm$ SD of three independent experiments each consisting of at least three replicates after negative control normalization. ($^{**}p<0.01$ and $^{*}p<0.02$ for UCHL3 and TIM).

as a product of PPP, and the changes in synthesis of F6P and G3P.

TIM is involved in glycolysis and gluconeogenesis, catalyzing the reversible interconversion of dihydroxyacetone phosphate (DHAP) and G3P. TIM has also been identified as a biomarker for hepatocellular carcinoma associated with hypoxia-inducible factor 1 α and for oxidative stress in rat retina under steroid-induced ocular hypertension [47, 48]. Studies conducted in lymphoblastoid cells and T lymphocytes suggest that the regulation of TIM gene expression can be modulated by biological response modifiers in plasma [49] and those T lymphocytes that undergo glutathionylation modulate the expression of TIM [50]. To date, no studies have evaluated the effect of DON exposure on rates of glycolysis and gluconeogenesis and TIM expression. The downregulation of TIM could lead to the impairment of glycolysis (and gluconeogenesis) and, subsequently, lead to reduced energy generation.

4.4 Regulation of transcription

DNA-directed RNA polymerases I, II and III subunit RPABC1 (RNA polymerases I, II and III subunit ABC1) were found to be upregulated by DON in RPMI 1788 cells. The products of RNA polymerases I, II and III are ribosomal RNA precursors, mRNA precursors and many functional non-coding RNAs and small RNAs, such as 5S rRNA and tRNAs, respectively [51].

To date, few studies have associated the activity of these polymerases with the development of diseases or their role in human lymphocyte function; so these effects of DON raise interesting new perspectives.

4.5 Validation

To confirm these changes of protein expression, we applied a flow cytometry approach to quantify effects on protein

expression. Although the most common approaches to confirm proteomic findings are Western blot and ELISA, flow cytometry has been widely used in immunology and is currently becoming more popular as a confirmation tool for proteomic approaches [52, 53]. Our results show that changes to protein expression can be detected using flow cytometry, therefore confirming the 2-DE findings, and reinforcing the intriguing association between DON exposure and its effects on previously highlighted cellular events.

4.6 Conclusions

This biomarker study on the effects of DON was developed based on the hypothesis that the proteome of treated human T and B lymphocyte cell lines would reflect the cellular effect of minimally toxic concentrations of DON. We have demonstrated that DON exposure affects the proteasome degradation pathway, metabolic processes such as carbohydrate and purine metabolism, transcription and cell integrity with different proteins affected in each cell line. Both T and B lymphocytes are components of the adaptive immune system, but playing somewhat different roles. Interestingly, we did not detect changes in the same proteins on both lymphocytes. Both cell lines have different origins: Jurkat E6.1 cells are derived from Jurkat FHCRC, which are leukemic T lymphocytes of human origin, and are able to produce IL-2 and IFN-γ or α while RPMI 1788 cells are derived from peripheral blood of an apparently healthy Caucasian male and secrete IgM. Furthermore, it is possible that DON has different targets in the two cell types thus potentially triggering different responses leading to varying proteome changes. The different sensitivity revealed after DON exposure (Fig. 1) shows that the significantly different origin and the distinct mechanistic functions of both cell lines may account for the lack of overlapping of proteins.

In association with the validation studies, our results suggest that the upregulation of the proteins that compose the proteasome degradation pathway may be associated with the activation of transcription factors and changes in cytokine expression proposed in the studies discussed previously. Moreover, our results also suggest that the upregulation in quantitative expression of IMDH2 and GMPS may influence the levels of glycine and its metabolism, the levels of GTP, which are essential for riboflavin metabolism and folate biosynthesis and the overall synthesis of RNA and DNA. Our results also suggest that the downregulation of TIM and TK may influence carbohydrate metabolism, namely phosphate pentose pathway, glycolysis and ultimately nucleotide metabolism. Therefore, it would be informative to investigate (i) the relationship between the effects of DON exposure and the series of proteins that activate the catalytic core of the proteasome and (ii) effects of DON exposure on the pool of nucleotides present in the pathway.

Although the quantitative changes in protein expression are low, they are likely to be meaningful taking into account the functional significance of the proteins identified (key modulators of cellular processes), supported by related published observations [54]. These results may reflect changes to other interrelated cellular events, which have not been seen before in respect to DON exposure. Therefore, our results reinforce the value of a panel of mechanism-based biomarkers over single proteins.

The next steps are to investigate to what extent DON exposure in vitro is reflected in primary cells as well as in vivo and whether the potential protein biomarkers identified can be applied to population-based studies of the effects of low dose, chronic DON exposure. Although we have conducted a systematic investigation focusing on a wide range of protein markers, the question remains as to whether other proteins (e.g. low-abundance proteins and phosphoproteins) will provide a more thorough understanding of the effects of DON exposure. Therefore, the present work could serve as the starting point for a deeper analysis of the immunomodulatory outcome of DON exposure on the human immune system.

We thank Dr. Werner Vos and Ms. Caroline Batchelor for assistance in using the nano-HPLC-Chip Ion Trap MS. Work was supported by the EU Integrated Project NewGeneris, 6th Framework Programme, Priority 5: Food Quality and Safety (Contract no. FOOD-CT-2005-016320; NewGeneris is the acronym of the project "Newborns and Genotoxic exposure risks" http://www.newgeneris.org) and a grant from the NIEHS, USA ES06052 to C. P. W.

The authors have declared no conflict of interest.

5 References

[1] Rotter, B. A., Prelusky, D. B., Pestka, J. J., Toxicology of deoxynivalenol (vomitoxin). *J. Toxicol. Environ. Health* 1996, *48*, 1–34.

[2] Young, L. G., McGirr, L., Valli, V. E., Lumsden, J. H., Lun, A., Vomitoxin in corn fed to young-pigs. *J. Anim. Sci.* 1983, *57*, 655–664.

[3] Iverson, F., Armstrong, C., Nera, E., Truelove, J. et al., Chronic feeding study of deoxynivalenol in B6C3F1 male and female mice. *Teratog. Carcinog. Mutagen.* 1995, *15*, 283–306.

[4] Sun, X. M., Zhang, X. H., Wang, H. Y., Cao, W. J. et al., Effects of sterigmatocystin, deoxynivalenol and aflatoxin G(1) on apoptosis of human peripheral blood lymphocytes in vitro. *Biomed. Environ. Sci.* 2002, *15*, 145–152.

[5] Meky, F. A., Hardie, L. J., Evans, S. W., Wild, C. P., Deoxynivalenol-induced immunomodulation of human lymphocyte proliferation and cytokine production. *Food Chem. Toxicol.* 2001, *39*, 827–836.

[6] Amuzie, C. J., Shinozuka, J., Pestka, J. J., Induction of suppressors of cytokine signaling by the trichothecene deoxynivalenol in the mouse. *Toxicol Sci.* 2009, *111*, 277–287.

[7] Pestka, J. J., Smolinski, A. T., Deoxynivalenol: toxicology and potential effects on humans. *J. Toxicol. Environ. Health B Crit. Rev.* 2005, *8*, 39–69.

[8] Li, F. Q., Li, Y. W., Luo, X. Y., Yoshizawa, T., *Fusarium* toxins in wheat from an area in Henan Province, PR China, with a previous human red mould intoxication episode. *Food Addit. Contam.* 2002, *19*, 163–167.

[9] Wild, C. P., Hall, A. J., in: Miller, H. (Ed.), *The Mycota VI. Human and Animal Relationships*, Springer, Berlin 1996, pp. 213–225.

[10] Pestka, J. J., Amuzie, C. J., Tissue distribution and proinflammatory cytokine gene expression following acute oral exposure to deoxynivalenol: comparison of weanling and adult mice. *Food Chem. Toxicol.* 2008, *46*, 2826–2831.

[11] Kim, E. J., Jeong, S. H., Cho, J. H., Ku, H. O. et al., Plasma haptoglobin and immunoglobulins as diagnostic indicators of deoxynivalenol intoxication. *J. Vet. Sci.* 2008, *9*, 257–266.

[12] Uzarski, R. L., Islam, Z., Pestka, J. J., Potentiation of trichothecene-induced leukocyte cytotoxicity and apoptosis by TNF-alpha and Fas activation. *Chem. Biol. Interact.* 2003, *146*, 105–119.

[13] Meky, F. A., Turner, P. C., Ashcroft, A. E., Miller, J. D. et al., Development of a urinary biomarker of human exposure to deoxynivalenol. *Food Chem. Toxicol.* 2003, *41*, 265–273.

[14] Turner, P. C., Burley, V. J., Rothwell, J. A., White, K. L. M. et al., Deoxynivalenol: rationale for development and application of a urinary biomarker. *Food Addit. Contam. Part A Chem. Anal. Control Expo. Risk Assess.* 2008, *25*, 864–871.

[15] Turner, P. C., Rothwell, J. A., White, K. L. M., Gong, Y. et al., Urinary deoxynivalenol is correlated with cereal intake in individuals from the United Kingdom. *Environ. Health Perspect.* 2008, *116*, 21–25.

[16] Severino, L., Russo, R., Luongo, D., De Luna, R. et al., Immune effects of four *Fusarium*-toxins (FB1, ZEA, NIV, DON) on the proliferation of Jurkat cells and porcine lymphocytes: in vitro study. *Vet. Res. Commun.* 2008, *32*, S311–313.

[17] Bartelt, R. R., Cruz-Orcutt, N., Collins, M., Houtman, J. C. D., Comparison of T cell receptor-induced proximal signaling and downstream functions in immortalized and primary T cells. *PLoS One* 2009, *4*, e5430.

[18] Khabar, K. S. A., al-Haj, L., al-Zoghaibi, F., Marie, M. et al., Expressed gene clusters associated with cellular sensitivity and resistance towards anti-viral and anti-proliferative actions of interferon. *J. Mol. Biol.* 2004, *342*, 833–846.

[19] Severino, L., Luongo, D., Bergamo, P., Lucisano, A., Rossi, M., Mycotoxins nivalenol and deoxynivalenol differentially modulate cytokine mRNA expression in Jurkat T cells. *Cytokine* 2006, *36*, 75–82.

[20] Volkova, O. Y., Reshetnikova, E. S., Mechetina, L. V., Chikaev, N. A. et al., Generation and characterization of monoclonal antibodies specific for human FCRLA. *Hybridoma* 2007, *26*, 78–85.

[21] Brambilla, F., Resta, D., Isak, I., Zanotti, M., Arnoldi, A., A label-free internal standard method for the differential analysis of bioactive lupin proteins using nano HPLC-Chip coupled with Ion Trap mass spectrometry. *Proteomics* 2009, *9*, 272–286.

[22] Sugita-Konishi, Y., Pestka, J. J., Differential upregulation of TNF-alpha, IL-6, and IL-8 production by deoxynivalenol (vomitoxin) and other 8-ketotrichothecenes in a human macrophage model. *J. Toxicol. Environ. Health A* 2001, *64*, 619–636.

[23] Kurihara, L. J., Kikuchi, T., Wada, K., Tilghman, S. M., Loss of UCH-L1 and UCH-L3 leads to neurodegeneration, posterior paralysis and dysphagia. *Hum. Mol. Genet.* 2001, *10*, 1963–1970.

[24] Kwon, J., Wang, Y. L., Setsuie, R., Sekiguchi, S. et al., Developmental regulation of ubiquitin C-terminal hydrolase isozyme expression during spermatogenesis in mice. *Biol. Reprod.* 2004, *71*, 515–521.

[25] Sano, Y., Furuta, A., Setsuie, R., Kikuchi, H. et al., Photoreceptor cell apoptosis in the retinal degeneration of UCHL3-deficient mice. *Am. J. Pathol.* 2006, *169*, 132–141.

[26] Rolen, U., Kobzeva, V., Gasparjan, N., Ovaa, H. et al., Activity profiling of deubiquitinating enzymes in cervical carcinoma biopsies and cell lines. *Mol. Carcinog.* 2006, *45*, 260–269.

[27] Shen, W. Y., Liu, H., Yu, Y. N., Translation initiation proteins, ubiquitin-proteasome system related proteins, and 14-3-3 proteins as response proteins in FL cells exposed to anti-benzo[a]pyrene-7,8-dihydrodiol-9,10-epoxide. *Proteomics* 2008, *8*, 3450–3468.

[28] Osman, A. M., Pennings, J. L. A., Blokland, M., Peijnenburg, A., van Loveren, H., Protein expression profiling of mouse thymoma cells upon exposure to the trichothecene deoxynivalenol (DON): implications for its mechanism of action. *J. Immunotoxicol.* 2010, *7*, 147–156.

[29] Wang, J., Maldonado, M. A., The ubiquitin-proteasome system and its role in inflammatory and autoimmune diseases. *Cell. Mol. Immunol.* 2006, *3*, 255–261.

[30] Karin, M., Delhase, M., The I kappa B kinase (IKK) and NF-kappa B: key elements of proinflammatory signalling. *Semin. Immunol.* 2000, *12*, 85–98.

[31] Girgis, G. N., Sharif, S., Barta, J. R., Boermans, H. J., Smith, T. K., Immunomodulatory effects of feed-borne *Fusarium* mycotoxins in chickens infected with coccidia. *Exp. Biol. Med.* 2008, *233*, 1411–1420.

[32] Zhou, H. R., Yan, D., Pestka, J. J., Induction of cytokine gene expression in mice after repeated and subchronic oral exposure to vomitoxin (deoxynivalenol): differential toxin-induced hyporesponsiveness and recovery. *Toxicol. Appl. Pharmacol.* 1998, *151*, 347–358.

[33] Gray, J. S., Pestka, J. J., Transcriptional regulation of deoxynivalenol-induced IL-8 expression in human monocytes. *Toxicol. Sci.* 2007, *99*, 502–511.

[34] van de Walle, J., Romier, B., Larondelle, Y., Schneider, Y.-J., Influence of deoxynivalenol on NF-kappaB activation and

IL-8 secretion in human intestinal Caco-2 cells. *Toxicol. Lett.* 2008, *177*, 205–214.

[35] Zhou, H. R., Islam, Z., Pestka, J. J., Rapid, sequential activation of mitogen-activated protein kinases and transcription factors precedes proinflammatory cytokine mRNA expression in spleens of mice exposed to the trichothecene vomitoxin. *Toxicol. Sci.* 2003, *72*, 130–142.

[36] Nyhan, W. L., Disorders of purine and pyrimidine metabolism. *Mol. Genet. Metab.* 2005, *86*, 25–33.

[37] Natsumeda, Y., Ohno, S., Kawasaki, H., Konno, Y. et al., Two distinct cDNAs for human IMP dehydrogenase. *J. Biol. Chem.* 1990, *265*, 5292–5295.

[38] Fellenberg, J., Bernd, L., Delling, G., Witte, D., Zahlten-Hinguranage, A., Prognostic significance of drug-regulated genes in high-grade osteosarcoma. *Mod. Pathol.* 2007, *20*, 1085–1094.

[39] Eugui, E. M., Allison, A. C., Immunosuppressive activity of mycophenolate mofetil. *Ann. N. Y. Acad. Sci.* 1993, *685*, 309–329.

[40] Quemeneur, L., Flacher, M., Gerland, L. M., Ffrench, M. et al., Mycophenolic acid inhibits IL-2-dependent T cell proliferation, but not IL-2-dependent survival and sensitization to apoptosis. *J. Immunol.* 2002, *169*, 2747–2755.

[41] Brouwer, C., Vermunt-de Koning, D. G. M., Trueworthy, R. C., ter Riet, P. et al., Monitoring of inosine monophosphate dehydrogenase activity in mononuclear cells of children with acute lymphoblastic leukemia: enzymological and clinical aspects. *Pediatr. Blood Cancer* 2006, *46*, 434–438.

[42] Vondersaal, W., Crysler, C. S., Villafranca, J. J., Positional isotope exchange and kinetic-experiments with escherichia-coli guanosine-5′-monophosphate synthetase. *Biochemistry* 1985, *24*, 5343–5350.

[43] Wamelink, M., Struys, E., Jakobs, C., The biochemistry, metabolism and inherited defects of the pentose phosphate pathway: a review. *J. Inherit. Metab. Dis.* 2008, *31*, 703–717.

[44] Paoletti, F., Mocali, A., Marchi, M., Truschi, F., Analysis of transketolase and identification of an enzyme variant in human-leukocytes. *Biochem. Biophys. Res. Commun.* 1989, *161*, 150–155.

[45] Pekovich, S. R., Martin, P. R., Singleton, C. K., Thiamine deficiency decreases steady-state transketolase and pyruvate dehydrogenase but not alpha-ketoglutarate dehydrogenase mRNA levels in three human cell types. *J. Nutr.* 1998, *128*, 683–687.

[46] Miccheli, A., Tomassini, A., Puccetti, C., Valerio, M. et al., Metabolic profiling by C-13-NMR spectroscopy: [1,2-C-13(2)] glucose reveals a heterogeneous metabolism in human leukemia T cells. *Biochimie* 2006, *88*, 437–448.

[47] Hamaguchi, T., Iizuka, N., Tsunedomi, R., Hamamoto, Y. et al., Glycolysis module activated by hypoxia-inducible factor 1 alpha is related to the aggressive phenotype of hepatocellular carcinoma. *Int. J. Oncol.* 2008, *33*, 725–731.

[48] Miyara, N., Shinzato, M., Yamashiro, Y., Iwamatsu, A. et al., Proteomic analysis of rat retina in a steroid-induced ocular hypertension model: potential vulnerability to oxidative stress. *Jpn. J. Ophthalmol.* 2008, *52*, 84–90.

[49] Ationu, A., Humphries, A., Layton, D. M., Regulation of triosephosphate isomerase (TPI) gene expression in TPI deficient lymphoblastoid cells. *Int. J. Mol. Med.* 1999, *3*, 21–24.

[50] Fratelli, M., Demol, H., Puype, M., Casagrande, S. et al., Identification by redox proteomics of glutathionylated proteins in oxidatively stressed human T lymphocytes. *Proc. Natl. Acad. Sci. USA* 2002, *99*, 3505–3510.

[51] Hiremath, C. N., Ladias, J. A. A., Expression and purification of recombinant hRPABC25, hRPABC17, and hRPABC14.4, three essential subunits of human RNA polymerases I, II, and III. *Protein Expr. Purif.* 1998, *13*, 198–204.

[52] Hor, S., Ziv, T., Admon, A., Lehner, P. J., Stable isotope labeling by amino acids in cell culture and differential plasma membrane proteome quantitation identify new substrates for the MARCH9 transmembrane E3 Ligase. *Mol. Cell. Proteomics* 2009, *8*, 1959–1971.

[53] Aggarwal, S., He, T., FitzHugh, W., Rosenthal, K. et al., Immune modulator CD70 as a potential cisplatin resistance predictive marker in ovarian cancer. *Gynecol. Oncol.* 2009, *115*, 430–437.

[54] Hopton, R. P., Turner, E., Burley, V. J., Turner, P. C., Fisher, J., Urine metabolite analysis as a function of deoxynivalenol exposure: an NMR-based metabolomics investigation. *Food Addit. Contam. Part A Chem. Anal. Control Expo. Risk Assess.* 2010, *27*, 255–261.

